Congestion Management in Distribution Networks With Asymmetric Block Offers

Hermann, Alexander Niels August; Kazempour, Jalal; Huang, Shaojun; Østergaard, Jacob

Published in:
IEEE Transactions on Power Systems

Link to article, DOI:
10.1109/TPWRS.2019.2912386

Publication date:
2019

Document Version
Peer reviewed version

Congestion Management in Distribution Networks With Asymmetric Block Offers

Alexander Hermann, *Student Member, IEEE,* Jalal Kazempour, *Senior Member, IEEE,* Shaojun Huang, *Senior Member, IEEE,* and Jacob Østergaard, *Senior Member, IEEE*

***Abstract*—In current practice, the day-ahead market-clearing outcomes are not necessarily feasible for distribution networks, i.e, the network constraints might not be satisfied. Hence, the distribution system operator may consider an ex-post re-dispatch mechanism, exploiting potential flexibility of local distributed energy resources (DERs) including demand response (DR) units. Many DR units have an inherent "rebound effect", meaning a decrease in power demand (response) must be followed by an increase (rebound) or vice-versa, due to their underlying physical properties. A naive re-dispatch mechanism relying on DR units with non-negligible rebound effect may fail, since those units may cause another congestion in the rebound period. We propose a mechanism, which models the rebound effect of DR units using asymmetric block offers — this way, those units offer their flexibility using two subsequent blocks (response and rebound), each one representing the load decrease/increase in a time period. We demonstrate that though linear approximations of optimal power flow (OPF) models as potential re-dispatch mechanisms are more computationally efficient, they can result in a different dispatch of the asymmetric blocks than an exact convex relaxation of an AC-OPF model, and therefore, must be used with caution.**

***Index Terms*—Congestion management, demand response, rebound effect, asymmetric block offers, convex relaxation.**

NOMENCLATURE

Sets and indices

C	Set of demand response units c
D	Set of offers d of each demand response unit
I	Set of distribution-level conventional generators i
L_n	Set of all facilities located at node n
N	Set of nodes n and j
PCC	Point of common coupling, i.e., the node connecting the distribution and transmission levels
T	Set of time steps t and τ
Φ_n	Set of all nodes connected to node n

Free Variables

p_{nt}/q_{nt}	Net active/reactive power injection at node n and time step t (positive for power injection) [kW/kVAr]
p_{njt}/q_{njt}	Active/reactive power flow from node n to j at time step t [kW/kVAr]

Non-negative Variables

$p_t^{\mathrm{up/dn,S}}$	Active power up/down-regulation provided by the transmission grid at time step t [kW]
$p_{it}^{\mathrm{up/dn}}$	Active power up/down-regulation provided by generator i at time step t [kW]
$q_t^{\mathrm{up/dn,S}}$	Reactive power up/down-regulation provided by the transmission grid at time step t [kVAr]
$q_{it}^{\mathrm{up/dn}}$	Reactive power up/down-regulation by generator i at time step t [kVAr]
$r_{dct}^{\mathrm{up/dn}}$	Active power up/down-regulation provided by demand response offer d of unit c at time step t [kW]
s_{tn}^{up}	Load curtailment at node n and time step t [kW]
v_{nt}	Squared voltage magnitude at node n and time step t [p.u.]
φ_{njt}	Squared current magnitude in line connecting node n to j [p.u.]

Binary Variables

o_{dct}	Activation of block d of demand response unit c at time step t

Parameters

A_{dc}	Orientation of offer d of demand response unit c. Equal to 1 if begins with up-regulation, equal to 0 otherwise
B_{nj}	Shunt susceptance of line connecting node n to j [p.u.]
$C_t^{\mathrm{p/q},\uparrow/\downarrow\mathrm{S}}$	Active/reactive up/down-regulation price provided from transmission level at the PCC at time step t [¢/kWh or ¢/kVArh]
$C_{dct}^{\mathrm{DR}\uparrow/\downarrow}$	Active power up/down-regulation offer price of demand response unit c, offer d, time t [¢/kWh]
C^{Shed}	Cost of load shedding [¢/kWh]
$C_{it}^{\mathrm{p/q},\uparrow/\downarrow}$	Active/reactive up/down-regulation offer price of conventional generator i at time step t [¢/kWh or ¢/kVArh]
D_{nt}^{disp}	Scheduled active power consumption of all inflexible loads at node n and time step t from the day-ahead market [kW]
DR_{ct}^{disp}	Scheduled active power consumption of demand response unit c at time step t from the day-ahead market [kW]
G_{nj}	Shunt conductance of line connecting node n to j [p.u.]
$\overline{F}_{nj}$	Capacity of line connecting node n to j [kVA]
$\overline{P}_i^{\mathrm{up/dn}}$	Maximum active power up/down-regulation capability of generator i [kW]
$\overline{P}^{\mathrm{up/dn,S}}$	Maximum active power up/down-regulation that can be provided by transmission level [kW]
$P_{dc}^{\mathrm{rsp/rb}}$	Response/rebound power of offer d of demand response unit c [kW]
P_{it}^{disp}	Dispatched active power production of generator i at time step t from the day-ahead market [kW]
P_{ct}^{cap}	Maximum active power consumption of demand response unit c at time step t [kW]
P_i^{cap}	Active power capacity of generator i [kW]
$\overline{Q}^{\mathrm{up/dn,S}}$	Maximum reactive power up/down-regulation that can be provided by transmission level [kVAr]
$\overline{Q}_i^{\mathrm{up/dn}}$	Maximum reactive power up/down-regulation capability of generator i [kVAr]
Q_{nt}	Total reactive power consumption at node n and time step t [kVAr]
R_{nj}	Resistance of line connecting node n to j [p.u.]
S_t^{disp}	Dispatched import/export of active power from the transmission system at time t from the day-ahead market [kW]
$T_{dc}^{\mathrm{rsp/rb/rec}}$	Response/rebound/recovery duration of demand response offer d of unit c [time step]
$\overline{V}_n^{\mathrm{sq}}$, $\underline{V}_n^{\mathrm{sq}}$	Upper and lower limits for voltage magnitude squared at node n [p.u.]
X_{nj}	Reactance of line connecting node n to j [p.u.]

A. Hermann, J. Kazempour and J. Østergaard are with the Technical University of Denmark, Kgs. Lyngby 2800, Denmark (email: alherm@elektro.dtu.dk; seykaz@elektro.dtu.dk; joe@elektro.dtu.dk).

S. Huang is with the University of Southern Denmark, Odense 5230, Denmark (email: shahu@mmmi.sdu.dk).

I. INTRODUCTION

IN current zonal electricity markets in Europe, the day-ahead market does not explicitly take into account the network constraints within zones. Therefore, the market-clearing outcomes are not necessarily feasible in terms of grid constraints. This brings challenges for both transmission and

distribution system operators (TSO and DSO), who are responsible for the secure and safe operation of their underlying systems. To resolve this issue, both TSO and DSO require flexible resources for congestion management and other uses, such as balancing and frequency control [1]. A significant part of such flexible resources is expected to be spread in distribution systems, in the form of distributed energy resources (DERs). These resources are able to provide flexibility to both TSO and DSO, and are also allowed to participate in the day-ahead market through new market players, such as aggregators and balancing responsible parties. Key is that the TSO and DSO need to coordinate how to use the DERs, ensuring both have access to flexible resources while operating their underlying system in a secure manner [2].

Different schemes have been recently proposed for TSO-DSO coordination [3]–[6], including suggestions for having either a common flexibility market for TSO and DSO, or separated markets. In some of those schemes, a bi-directional but non-iterative communication between DSO and TSO is required, in which the DSO shares its feasible region with the TSO [7]. Some other schemes suggest maintaining the current uni-directional communication in which the TSO is not coordinated with the DSO, but the DSO needs ex-post actions. Ex-post here means that the DSO re-dispatches local DERs using a bid-based auction with day-ahead dispatches as inputs. This mechanism uses local flexible resources for congestion management and resolving nodal voltage issues [8]. The focus of this paper is an ex-post method.

Demand response (DR) units are expected to provide a large share of the DER penetration in distribution grids. Many DR units, especially thermostatically controlled loads, exhibit an inherent *rebound (kick-back) effect* because of their underlying physical properties [9]. It means that any load decrease/increase in a specific time period (response) may be followed by a load increase/decrease in the subsequent time period (rebound) [10]. This effect complicates any problem including DR units, since it makes the future load profile *decision-dependent* (i.e. not exogenous anymore). One natural approach to model rebound effect is dynamic programming, such that the dispatch of DR unit at time step k affects load level at time steps $t > k$ [11]. However, dynamic programming with iterative solution techniques is not compatible with existing market-clearing frameworks[1]. Therefore, other alternatives are needed to model rebound effects within market frameworks, e.g., new offering formats for DR units [12]. One appealing market-compatible concept is *asymmetric block offers* [13], which include two parts, response and rebound. Each part models either load increase or decrease. One can view the combination of these two parts as a load shifting offer in time, but without a time gap between response and rebound time periods. We use the concept of asymmetric block offers, because it allows us to model rebound *a priori* in our market model without the need for an iterative clearing process. However, these block offers may bring computational challenges due to additional binary variables required for modeling the blocks[2]. Detailed description of these offers will be provided in the following section.

There is an extensive literature on congestion management in distribution networks using DR units - see [8] for a relevant survey. The two main strategies to reward those units are: i) the price-based methods [15]–[17], where DR units participate in any mechanism as individual profit-maximizing players, and ii) the incentive-based methods, where DR units are paid based on pre-defined incentive rates [18]–[20]. The key point is that all these papers ignore the potential rebound effect of DR units, while this may incur another congestion in the coming time steps, or overestimate the capability of DR units to effectively help the DSO with congestion management.

In this paper, the main technical question is: how should an appropriate DSO-level congestion management mechanism be implemented, while accurately accounting for rebound effects of local DR units? This underlying mechanism is to be solved by the DSO once the day-ahead market is cleared. Therefore, the day-ahead dispatch of local resources is given, and goal of the proposed mechanism is to optimally adjust those resources for meeting local distribution network constraints at the minimum re-dispatch cost. The important constraints to be fulfilled in the re-dispatch mechanism include nodal voltage and line flow limits in the distribution network. In addition, it is of importance to consider power losses in the distribution grid. This raises another technical question: To what extent should the distribution grid constraints and losses be taken into account in the re-dispatch mechanism, and how sensitive are the re-dispatch results to those considerations?

Our first contribution is to develop a re-dispatch mechanism for a DSO as an ex-post congestion management action, while accounting for rebound effects of DR units a priori using asymmetric block offers. To the best of our knowledge, [13] is the only paper in existing literature incorporating the rebound effects in a compatible way into a balancing market framework. However, it ignores network representation, which is essential in any distribution-level mechanism, including the congestion management mechanism in our study. The full grid representation of a distribution system is a non-convex problem with optimality and computational challenges. This becomes worse when adding binary variables due to the representation of blocks. Our second contribution is to provide a comprehensive analysis to explore how different grid representations change the re-dispatch outcomes and the computational burden. In particular, to investigate how distribution network simplifications, as is common in practice, influence the re-dispatch results, we develop three distribution optimal power flow (OPF) models. Each model has increasing accuracy. The more accurate model is indeed the more complex one, which is computationally more expensive. Accounting for the rebound effects, two models are mixed-integer linear programming (MILP) problems (one without and one with loss approximations), while the last one is a mixed-integer second order cone problem (MI-SOCP). The latter model is a convex conic relaxation of the original AC-OPF model, which performs

[1]The current markets prefer non-iterative clearing mechanisms with straightforward, easy-to-implement and transparent clearing mechanisms.

[2]Adding block offers is common place in European zonal electricity markets, as conventional generators are allowed to submit different types of block offers to ensure their internal unit commitment constraints [14].

well in radial networks [21], [22]. To ensure exactness of the convex relaxation we also present some sufficient conditions for exactness and show some of the implications of using those conditions [21], [23]. Our study shows that the MILP models are computationally faster, which makes them suitable to be used in practice. However, they do not necessarily obtain identical re-dispatch results to those in the MI-SOCP model, which solves the problem in our study around 4 to 7 times slower without sufficient conditions for exactness, and 7 to 60 times slower if those conditions are added. Therefore, MILP versions of this re-dispatch mechanism are practical but must be used with caution.

The rest of the paper is structured as following: Section II describes the implementation of asymmetric block offers, and explains the congestion management mechanism. Section III proposes the congestion management method using three different OPF models. Section IV provides results for two case studies. Concluding remarks are given in Section V.

II. Congestion Management using Asymmetric Block Offers

This section describes the details of asymmetric block offers, and the framework of the proposed congestion management mechanism.

A. Asymmetric Block Offers

Examples of some potential flexible loads that exhibit a rebound effect are refrigeration units, water heaters and heat pumps with storage for building temperature control. They can be used as DR units, by deviating from a base-line temperature setting and approaching either an upper or a lower allowable temperature threshold. When the temperature threshold is reached, DR units have to increase (or decrease) their power consumption for a period, in order to return to the base-line setting [9], [10]. The time to reach the upper or lower temperature thresholds can be found by thermal modeling of the underlying system. The time period from DR activation until reaching the temperature threshold is referred to as *response* period, while the subsequent time period until returning to the base-line setting is referred to as *rebound* period [13]. An asymmetric block offer models the response and rebound parts of the DR unit. This type of offer allows exploiting demand-side flexibility by directly modeling temporal load shifting in the dispatch mechanism. These block offers can be designed as shown in Fig. 1, where two examples are plotted with different order of up- and down-regulation directions. By asymmetric, it means that they can have different power consumption levels and duration for response and rebound parts. The asymmetric block offers are indeed the market offers of DR units or flexibility aggregators in general. It is up to the flexibility aggregators to ensure that the block offers are technically feasible. Since this paper looks at the problem from a DSO perspective, the asymmetric block offers are exogenous, and their synthesis are out of the scope of this paper[3]. However, in general, these offers can be derived by approximation models (e.g. ARMAX model [25]) using measurement data from thermal test units.

[3]We refer the interested readers to [24] for offering strategy problem of DR units and flexibility aggregators using asymmetric block offers.

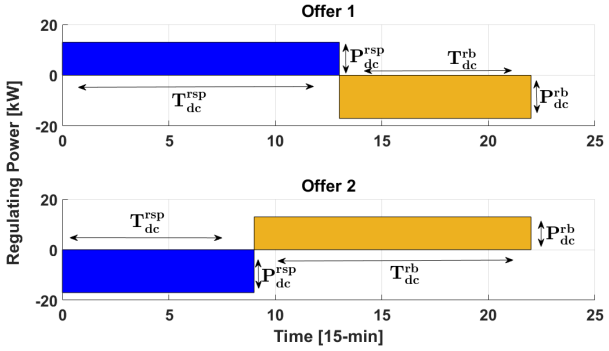

Fig. 1. Two examples of possible asymmetric block offers for a demand response unit. A positive/negative regulating power corresponds to up/down-regulation, respectively. In Offer 1 (upper plot), the response part (in blue) provides up-regulation, i.e., a decrease in load power consumption. Its rebound (in yellow) corresponds to a subsequent load increase, i.e. down regulation. Further, Offer 2 (lower plot) includes down- and up-regulation in response and rebound parts, respectively.

B. Congestion Management: Framework and Assumptions

The outcome of the day-ahead market does not necessarily respect the DSO-level network constraints. When the day-ahead market dispatch does not respect the constraints in the distribution network, the most cost-efficient way is to resolve these violations locally. Distribution network congestion will be one of the prime issues in the future, due to increased line loading, with the expected large scale deployment of distributed photovoltaic power and battery storage. Often congestion will be coupled with voltage limit violations, therefore it is also important to model that aspect of the grid. This paper proposes an ex-post mechanism to be run *right after* the day-ahead market, which is performed locally by the DSO. The DSO uses a market-based solution to determine the optimal re-dispatch actions, while obtaining the minimum total re-dispatch cost. According to the market-clearing outcomes, the DSO pays the DERs. Since the largest volume of the DR units with rebound characteristics are generally located in radial distribution feeders, it is logical to use their load-shifting potential to resolve local issues.

Any DSO-level congestion management mechanism should take as *input* the results of the day-ahead market clearing, as this comprises the power settings of the flexible loads and distributed generation. The DSO uses these values to determine whether there are any issues with congestion and/or voltage limit violations within the distribution network. If any issues are detected, the DSO requests offers for down- and up-regulation from the individual DR units, local conventional generators and flexibility aggregators. These offers can be in the form of conventional offers by local dispatchable generators or of asymmetric block offers by local DR units. Also, the TSO is viewed as a flexibility provider through TSO-level flexible resources but potentially at a higher cost. However,

note that the change of the import/export at the PCC[4] is limited by lower and upper bounds ($\overline{P}^{\mathrm{dn,S}}$ and $\overline{P}^{\mathrm{up,S}}$). Indeed, the TSO provides this limited flexibility by activation of reserve capacity from TSO-level flexible resources without need for changing the day-ahead market outcomes [5].

After collecting the submitted offers, the DSO runs the congestion management mechanism, whose objective is to meet local constraints at the minimum re-dispatch cost. In addition, the outcomes are accepted offers for up- and down-regulation. Regarding the potential uncertainty sources, e.g., load and renewable power uncertainties, we assume that they have been already considered during the day-ahead market clearing. Therefore, the proposed ex-post re-dispatch mechanism does not need to model again those uncertainties. Moreover, the DSO may be unwilling to collect and manipulate statistical data in order to model future uncertainties, because in current market frameworks this duty falls to the market operator.

Since the DSO-level network is usually radial, a congested line can only be relieved, if any resources on both sides of that line are available for re-dispatch. This is because any up-regulation somewhere in the network has to be matched by an equal down-regulation elsewhere (minus line losses). One important observation is that the accepted offers for up- and down-regulation should be located on both sides of the congested line, in order to maintain power balance. The DR units furthest away from the PCC are the ones that are most likely to be scheduled, when congestion occurs.

III. Mathematical Model

Section III-A provides the mathematical representation of asymmetric block offers. Afterwards, Section III-B includes asymmetric block offers within three proposed OPF models as alternative congestion management mechanisms with different levels of complexity.

A. Mathematical Representation of Asymmetric Block Offers

This section provides a modified version of formulations for asymmetric block offers from [13], yielding a set of mixed-integer linear inequalities. These conditions will be included in Section III-B as constraints of OPF models. Asymmetric block offers beginning with up-regulation response, e.g., Offer 1 in Fig. 1, are modeled by equations (1), while offers beginning with down-regulation response, e.g., Offer 2 in Fig. 1, are represented by equations (11) in the online appendix [26]. These two different kinds of block offers are differentiated by binary parameter A_{dc}. If A_{dc} is set to 1, it indicates that block offer d of unit c begins with up-regulation, or to 0 if it begins with down-regulation. The binary variable o_{dct} is a decision variable to activate a given offer d from DR unit c in time step t.

$$\Big\{ r^{\mathrm{up}}_{dct} \le P^{\mathrm{rsp}}_{dc} o_{dct}, \quad \forall d,c,t \tag{1a}$$

$$r^{\mathrm{dn}}_{dct} \le P^{\mathrm{rb}}_{dc} o_{dct}, \quad \forall d,c,t \tag{1b}$$

$$\sum_{\tau=t}^{t+T^{\mathrm{rsp}}_{dc}-1} r^{\mathrm{up}}_{dc\tau} \ge T^{\mathrm{rsp}}_{dc} P^{\mathrm{rsp}}_{dc}(o_{dct} - o_{dc,t-1}), \quad \forall d,c,t \tag{1c}$$

$$\sum_{\tau=t+T^{\mathrm{rsp}}_{dc}}^{t+T^{\mathrm{rsp}}_{dc}+T^{\mathrm{rb}}_{dc}-1} r^{\mathrm{dn}}_{dc\tau} \ge T^{\mathrm{rb}}_{dc} P^{\mathrm{rb}}_{dc}(o_{dct} - o_{dc,t-1}), \quad \forall d,c,t \le |T| - T^{\mathrm{rsp}}_{dc} \tag{1d}$$

$$\sum_{\tau=t}^{t+T^{\mathrm{rsp}}_{dc}-1} r^{\mathrm{dn}}_{dc\tau} \le T^{\mathrm{rb}}_{dc} P^{\mathrm{rb}}_{dc}(1-(o_{dct} - o_{dc,t-1})), \forall d,c,t \tag{1e}$$

$$\sum_{\tau=t+T^{\mathrm{rsp}}_{dc}}^{t+T^{\mathrm{rsp}}_{dc}+T^{\mathrm{rb}}_{dc}-1} r^{\mathrm{up}}_{dc\tau} \le T^{\mathrm{rsp}}_{dc} P^{\mathrm{rsp}}_{dc}(1-(o_{dct} - o_{dc,t-1})) \tag{1f}$$

$$, \forall d,c,t \le |T| - T^{\mathrm{rsp}}_{dc} \Big\} \text{ if } A_{dc} = 1.$$

Conditions (1a) and (1b) restrict up- and down-regulation r^{up}_{dct} and r^{dn}_{dct} to the prescribed magnitude of response P^{rsp}_{dc} and rebound P^{rb}_{dc}, respectively. In (1c), the length of the response, if offer d is activated, is set to the prescribed response time T^{rsp}_{dc}. Condition (1d) is similar to (1c), but for the rebound part of the block offer. Note that $|T|$ indicates the cardinality of set T. Condition (1e) ensures that variable r^{dn}_{dct} is 0 during up-regulation. Similarly, condition (1f) imposes $r^{\mathrm{up}}_{dct} = 0$ during down-regulation.

In addition to (1) and (11), a minimum recovery period, if exists, needs to be enforced. This condition is enforced by (2). Parameter T^{rec}_{dc} corresponds to the recovery time between the two consecutive asymmetric block offers (not between response and rebound parts of a block offer). In other words, it enforces the minimum recovery time between the rebound part of one block and the response part of the next block.

$$\sum_{\tau=t+T^{\mathrm{resp}}_{dc}+T^{\mathrm{reb}}_{dc}}^{t+T^{\mathrm{resp}}_{dc}+T^{\mathrm{reb}}_{dc}+T^{\mathrm{rec}}_{dc}-1} (1-o_{dc,\tau}) \ge T^{\mathrm{rec}}_{dc}(o_{dct} - o_{dct-1})$$
$$, \forall d,c,t \le |T| - (T^{\mathrm{resp}}_{dc} + T^{\mathrm{reb}}_{dc}) + 1. \tag{2}$$

In (3), it is ensured that each DR unit is only able to activate at most one block offer in any time step:

$$\sum_{d} o_{dct} \le 1, \quad \forall c,t. \tag{3}$$

The asymmetric block offers also need to be finished before the end of the planning horizon, such that the whole block offer is realized before the planning horizon. Condition (4) ensures that the entire asymmetric block offer is dispatched within the time horizon considered, e.g., 24 hours. For example, this constraint makes sure that there is no case in which the response part is dispatched in the upcoming 24 hours, while its rebound part is allocated in the beginning hours of the subsequent day.

$$1 - (o_{dc,t+1} - o_{dct}) \le 2(1 - o_{dc|T|})$$
$$, \forall d,c,t = |T| - (T^{\mathrm{resp}}_{dc} + T^{\mathrm{reb}}_{dc}). \tag{4}$$

B. Congestion Management Mechanism: OPF Models

Accounting for rebound effect of DR units, this subsection provides three different alternatives for DSO-level congestion management, with increasing levels of accuracy and therefore complexity. The first model is the simplest one, which is a linear DC-OPF problem for radial distributions systems,

[4]The point of common coupling, i.e. the transformer substation which connects the distribution and transmission networks.

ignoring losses while decoupling active and reactive power flows. The second one improves the first model by adding a loss approximation for active power flows via cuts, but at the cost of using an iterative process [27], [28]. As the most accurate alternative among the three OPF models used in this paper, the third one is an SOCP, which takes into account losses for both active and reactive power flows[5] [29]. All these three models will be mixed-integer programs due to binary variables in (1)-(4) and (11).

The objective function of all three OPF models used in this paper is the same as given in (5). It minimizes the total re-dispatch cost, which is a linear combination of the costs for up- and down-regulation[6] of active and reactive power from different sources, i.e. TSO, local conventional generators i, DR units c and involuntary curtailment of loads.

$$\begin{aligned}\min_{\Xi} \quad f(\Xi) = \sum_t \Big[& \underbrace{C_t^{\mathrm{p}\uparrow\mathrm{S}} p_t^{\mathrm{up,S}}}_{\text{Cost of } p^{\mathrm{up}} \text{ from TSO}} - \underbrace{C_t^{\mathrm{p}\downarrow\mathrm{S}} p_t^{\mathrm{dn,S}}}_{\text{cost of } p^{\mathrm{dn}} \text{ to TSO}} \\ & + \underbrace{C_t^{\mathrm{q}\uparrow\mathrm{S}} q_t^{\mathrm{up,S}}}_{\text{Cost of } q^{\mathrm{up}} \text{ from TSO}} - \underbrace{C_t^{\mathrm{q}\downarrow\mathrm{S}} q_t^{\mathrm{dn,S}}}_{\text{Cost of } q^{\mathrm{dn}} \text{ to TSO}} \Big] + \sum_{n,t} \Big[\underbrace{C^{\mathrm{Shed}} s_{nt}^{\mathrm{up}}}_{\text{Curtailment cost}} \Big] \\ & + \sum_{i,t} \Big[\underbrace{C_{it}^{\mathrm{p}\uparrow} p_{it}^{\mathrm{up}}}_{\text{Cost of } p^{\mathrm{up}} \text{ from gen.}} - \underbrace{C_{it}^{\mathrm{p}\downarrow} p_{it}^{\mathrm{dn}}}_{\text{Cost of } p^{\mathrm{dn}} \text{ to gen.}} + \underbrace{C_{it}^{\mathrm{q}\uparrow} q_{it}^{\mathrm{up}}}_{\text{Cost of } q^{\mathrm{up}} \text{ from gen.}} \\ & - \underbrace{C_{it}^{\mathrm{q}\downarrow} q_{it}^{\mathrm{dn}}}_{\text{Cost of } q^{\mathrm{dn}} \text{ to gen.}} \Big] + \sum_{d,c,t} \Big[\underbrace{C_{dct}^{\mathrm{DR}\uparrow} r_{dct}^{\mathrm{up}}}_{\text{Cost of } r^{\mathrm{up}} \text{ from DR}} - \underbrace{C_{dct}^{\mathrm{DR}\downarrow} r_{dct}^{\mathrm{dn}}}_{\text{Cost of } r^{\mathrm{dn}} \text{ to DR}} \Big] \end{aligned} \tag{5}$$

where Ξ is the set of optimization variables, including free variables p_{nt}, q_{nt}, p_{njt}, q_{njt}, non-negative variables p_{it}^{up}, p_{it}^{dn}, r_{dct}^{up}, r_{dct}^{dn}, s_{nt}^{up}, $p_t^{\mathrm{up,S}}$, $p_t^{\mathrm{dn,S}}$, q_{it}^{up}, q_{it}^{dn}, $q_t^{\mathrm{up,S}}$, $q_t^{\mathrm{dn,S}}$, v_{nt}, and binary variables o_{dct}.

The common constraints for all three OPF models are given in (6). Note that DR_{ct}^{disp}, D_{nt}^{disp}, S_t^{disp} and P_{it}^{disp} are parameters, indicating day-ahead market outcomes.

$$p_{nt} = \sum_{j\in\Phi_n} p_{njt}, \quad \forall n,t \tag{6a}$$

$$q_{nt} = \sum_{j\in\Phi_n} q_{njt}, \quad \forall n,t \tag{6b}$$

$$\begin{aligned} p_{nt} = & \sum_{d,c\in L_n} [r_{dct}^{\mathrm{up}} - r_{dct}^{\mathrm{dn}}] - \sum_{c\in L_n} DR_{ct}^{\mathrm{disp}} \\ & + \sum_{i\in L_n} \left[p_{it}^{\mathrm{up}} - p_{it}^{\mathrm{dn}} + P_{it}^{\mathrm{disp}} \right] \\ & + \left[S_t^{\mathrm{disp}} + p_t^{\mathrm{up,S}} - p_t^{\mathrm{dn,S}} \right]_{n\in PCC} \\ & - D_{nt}^{\mathrm{disp}} + s_{nt}^{\mathrm{up}} - \sum_{j\in\Phi_n} \frac{G_{nj}}{2} v_{nt}, \quad \forall n,t \end{aligned} \tag{6c}$$

$$\begin{aligned} q_{nt} = & \sum_{i\in L_n} \left[q_{it}^{\mathrm{up}} - q_{it}^{\mathrm{dn}} \right] + \left[q_t^{\mathrm{up,S}} - q_t^{\mathrm{dn,S}} \right]_{n\in PCC} \\ & - Q_{nt} + \sum_{j\in\Phi_n} \frac{B_{nj}}{2} v_{nt}, \ \forall n,t \end{aligned} \tag{6d}$$

$$\sum_d r_{dct}^{\mathrm{up}} \le DR_{ct}^{\mathrm{disp}}, \quad \forall c,t \tag{6e}$$

$$p_{it}^{\mathrm{dn}} \le P_{it}^{\mathrm{disp}}, \quad \forall i,t \tag{6f}$$

$$s_{nt}^{\mathrm{up}} + \sum_{d,c\in L_n} \left[r_{dct}^{\mathrm{up}} - r_{dct}^{\mathrm{dn}} \right] \le D_{nt}^{\mathrm{disp}} + \sum_{c\in L_n} DR_{ct}^{\mathrm{disp}}, \forall n,t \tag{6g}$$

$$p_{it}^{\mathrm{up}} + P_{it}^{\mathrm{disp}} \le P_i^{\mathrm{cap}}, \quad \forall i,t \tag{6h}$$

$$\sum_d r_{dct}^{\mathrm{dn}} + DR_{ct}^{\mathrm{disp}} \le P_{ct}^{\mathrm{cap}}, \quad \forall c,t \tag{6i}$$

$$p_{it}^{\mathrm{up}} \le \overline{P}_i^{\mathrm{up}}, \ p_{it}^{\mathrm{dn}} \le \overline{P}_i^{\mathrm{dn}}, \ \forall i,t \tag{6j}$$

$$q_{it}^{\mathrm{up}} \le \overline{Q}_i^{\mathrm{up}}, \ q_{it}^{\mathrm{dn}} \le \overline{Q}_i^{\mathrm{dn}}, \quad \forall i,t \tag{6k}$$

$$p_t^{\mathrm{up,S}} \le \overline{P}^{\mathrm{up,S}}, \ p_t^{\mathrm{dn,S}} \le \overline{P}^{\mathrm{dn,S}}, \ \forall t \tag{6l}$$

$$q_t^{\mathrm{up,S}} \le \overline{Q}^{\mathrm{up,S}}, \ q_t^{\mathrm{dn,S}} \le \overline{Q}^{\mathrm{dn,S}}, \ \forall t \tag{6m}$$

$$\underline{V}_n^{\mathrm{sq}} \le v_{nt} \le \overline{V}_n^{\mathrm{sq}}, \quad \forall n,t. \tag{6n}$$

The net active and reactive power injection at node n is linked to corresponding flow from node n to j in (6a) and (6b). The nodal active power balance is enforced by (6c). Note that the last term of (6c) takes into account the shunt conductance of the lines[7]. The nodal reactive power balance is enforced by (6d), which also takes into account the shunt susceptance of the lines connected to node n. The up-regulation (load decrease) provided by DR unit c is limited to its scheduled consumption DR_{ct}^{disp} in (6e). The down-regulation (generation decrease) provided by generator i is restricted to its dispatch from the day-ahead market by (6f). Constraint (6g) limits the curtailed load s_{nt}^{up} according to total scheduled consumption of flexible and inflexible loads from the day-ahead market and provided regulation from DR units. The up-regulation (generation increase) provided by conventional generator i is limited by (6h). Similarly, (6i) restricts the down-regulation (load increase) provided by DR unit c. Constraints (6j) and (6k) limit the active and reactive power regulation of conventional generator i to its maximum capability. Similar constraints are applied to the import/export at the PCC from transmission level in (6l) and (6m). Constraint (6n) limits the voltage magnitude to the upper and lower thresholds.

1) Mixed-Integer Linear OPF (Lossless): The lossless mixed-integer linear OPF is the simplest approximation of the power flow for radial distribution systems used in this paper. It is possible by using this OPF method to include the line congestion and voltage issues. Similar to LinDistFlow model in [30], in order to have an approximation of both active and reactive power flow and their effect on the voltage, a decoupled linear power flow is used. The advantage of this approach is that it is computationally simple and well known. For the radial case, the linearized branch flow OPF boils down to problem (7):

$$\min_{\Xi} \ f(\Xi) \text{ as in (5)} \tag{7a}$$

subject to:

[5]The original AC-OPF model is a non-convex quadratically constrained program [29], which can be convexified by relaxing it to either an SOCP or a semi-definite program. We use the former in this paper.

[6]The DSO pays for up-regulation, while it is paid by sources providing down-regulation.

[7]Half of the shunt losses due to shunt admittance of every line connected to node n is subtracted from that node. In general, shunt conductance of lines is small and can be ignored. However, shunt susceptance can be significant in underground cables.

$$p_{njt} = -p_{jnt},\ q_{njt} = -q_{jnt},\ \forall n, j \in \Phi_n, t \quad (7b)$$
$$\sum_n p_{nt} = 0, \quad \forall t \quad (7c)$$
$$\sum_n q_{nt} = 0, \quad \forall t \quad (7d)$$
$$p_{njt} \le \overline{F}_{nj}, \quad \forall n, j \in \Phi_n, t \quad (7e)$$
$$v_{jt} = v_{nt} - 2\left(R_{nj}p_{njt} + X_{nj}q_{njt}\right), \forall n, j \in \Phi_n, t \quad (7f)$$
(1) to (4), (6) and (11). (7g)

Constraints (7b), (7c) and (7d) model the lossless linear power flow. To preserve linearity, (7e) imposes the line capacity limit in terms of active power flow only. Finally, (7f) links the voltage magnitude of two adjacent nodes with impedance and power flows as a linear approximation. Similar to [30], a variable v_{nt} is introduced to present squared voltage magnitude, such that the model remains linear.

2) Mixed-Integer Linear OPF With Losses: The mixed-integer linear OPF model (7) does not take into account losses. In order to improve the accuracy of the congestion management method, it is desirable to model losses, especially for low-voltage radial systems with relatively large losses. An approximation of active power losses is slightly more complex, since losses generally are quadratic to the flow in a line. In order to keep the model linear, an iterative approach as in [27] and [28] can be used. For every iteration of solving the OPF problem a new *loss-cut* is generated, which approximates the losses successively. This approach usually converges after very few iterations. The loss in a line that can be assigned to a node is approximated by (8) [27]:

$$P_{nt}^{\text{loss,fix}} = \sum_{j\in\Phi_n}\left(\frac{R_{nj}\ p_{njt}^2}{2}\right),\ \forall n, t. \quad (8)$$

Here the losses are a quadratic function of the line flows. The procedure used in [27] is then to add half of the losses to the consumption of every node connected to the ends of the line. In order for the losses to be at the lower bound of the loss-cut at iteration ν, an auxiliary slack variable $y_{nt}^{(\nu)}$ is added to the objective function, but at a negligible small profit C^y. The mixed-integer linear OPF problem at iteration ν including the loss-cuts is given in optimization problem (9):

$$\min_{\Xi, y_{nt}^{(\nu)}\ge 0, p_{nt}^{\text{loss}(\nu)}\ge 0} \quad f(\Xi)^{(\nu)} - \sum_{nt} C^y y_{nt}^{(\nu)} \quad (9a)$$
subject to:
$$\sum_n (p_{nt}^{(\nu)} - p_{nt}^{\text{loss}(\nu)} - y_{nt}^{(\nu)}) = 0,\ \forall t \quad (9b)$$
$$p_{nt}^{(\nu)} - p_{nt}^{\text{loss}(\nu)} - y_{nt}^{(\nu)} = \sum_{j\in\Phi_n} p_{njt}^{(\nu)},\ \forall n, t \quad (9c)$$
$$p_{nt}^{\text{loss}(\nu)} - \sum_{j\in\Phi_n}(R_{nj}\ P_{njtr}^{\text{fix}})p_{njt}^{(\nu)} \ge -P_{ntr}^{\text{loss,fix}}, \forall n, t, r = \{1, \dots, \nu-1\} \quad (9d)$$
(1) to (4), (6b) to (6n), (7b),(7d), (7e), (7f) and (11) (9e)

where r is the index of loss-cuts, and parameter $P_{ntr}^{\text{loss,fix}}$ is the fixed loss obtained from the line flow of the previous iterations by solving (8). Furthermore, parameter P_{njtr}^{fix} is the flow in the line connecting nodes n and j from the previous iterations. The problem (9) has to be solved iteratively, adding one cut per iteration in (9d). The convergence is reached at iteration ν once $\left|\sum_{nt} P_{nt,(r=\nu)}^{\text{loss,fix}} - \sum_{nt} p_{nt}^{\text{loss},(\nu)}\right| \le \epsilon$, where ϵ is a small tolerance. Note that the optimal value of slack variable $y_{nt}^{(\nu)}$ should be zero.

3) Mixed-Integer SOCP-OPF: The mixed-integer SOCP OPF model for radial distribution systems is presented in (10) [29]:

$$\min_{\Xi, \varphi_{njt}\ge 0} f(\Xi) \text{ as in (5)} \quad (10a)$$
subject to:
$$p_{njt}^2 + q_{njt}^2 \le \varphi_{njt} v_{nt},\ \forall n, j \in \Phi_n,\ t \quad (10b)$$
$$p_{njt} + p_{jnt} = R_{nj}\varphi_{njt},\ \forall n, j \in \Phi_n,\ t \quad (10c)$$
$$q_{njt} + q_{jnt} = X_{nj}\varphi_{njt},\ \forall n, j \in \Phi_n,\ t \quad (10d)$$
$$v_{jt} = v_{nt} - 2(R_{nj}p_{njt} + X_{nj}q_{njt}) + (R_{nj}^2 + X_{nj}^2)\varphi_{njt}, \forall n, j \in \Phi_n,\ t \quad (10e)$$
$$p_{njt}^2 + q_{njt}^2 \le \overline{F}_{nj}^2,\ \forall n, j \in \Phi_n,\ t \quad (10f)$$
(1) to (4), (6) and (11). (10g)

Constraint (10b) is a convex relaxation of a quadratic equality constraint from the original non-convex AC-OPF problem. This relaxation is necessary to include the interior space of the quadratic cone described by this equation to ensure convexity. Constraints (10c) and (10d) are the active and reactive power losses, respectively. Constraint (10e) relates the voltage drop to the power flows and currents. In (10f) the line flow limit is enforced. In our numerical studies, the sufficient conditions introduced in [21] are also added to (10) to ensure zero duality gap (i.e., exactness) of the relaxation in radial networks[8]. These sufficient conditions are given in the online appendix [26]. Note that these conditions guarantee achieving the exactness, but at the cost of shrinking the feasible space, and potentially increasing the system cost and usually the computational burden.

IV. Case Studies

An illustrative example and a larger case study using the IEEE 37-node test feeder are provided. All cases are implemented in GAMS and solved using CPLEX version 12.8.

A. Illustrative Example

A radial 6-node system is used to introduce the congestion management mechanism with different OPF models. The diagram of this feeder is illustrated in Fig. 2. This feeder contains three DR units (c_1 to c_3) and two local conventional generators (i_1 and i_2). The line connecting nodes 3 and 4 is likely to be congested due its limited capacity (40 kVA). All line resistances are set to 0.001 p.u. and reactances are fixed to 0.0005 p.u. In addition, the shunt conductance and susceptance of all lines are set to be 0.1 p.u. As input

[8]Without sufficient conditions, the second-order cone constraint (10b) might be still binding in specific cases (e.g., in the case studies of this paper presented in Section IV), but there is no exactness guarantee in general. In case of inexactness, an ex-post procedure for feasibility recovery is required [31].

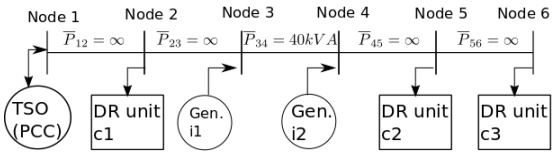

Fig. 2. Illustrative example: 6-node radial feeder.

parameters, the global day-ahead market outcomes are given in the online appendix [26] (particularly, see Fig. 9 in that appendix). This figure includes 40 time steps, with resolution of 15 minutes. These inputs from the day-ahead dispatches makes the line connecting nodes 3 and 4 overloaded by 23 kVA throughout the time periods 12 to 26, and the DSO needs to run the proposed congestion management mechanism to relieve congestion using local flexible resources (two generators and three DR units) as well as changing the import/export from/to the TSO. Each local generator can provide active power up- and down-regulation up to 80 kW, and reactive power up- and down-regulation up to 30 kVAr. These limits for TSO are 100 kW and 30 kVAr. Each of the three DR units is offering four different asymmetric block offers (d_1 to d_4) as given in the online appendix [26] (in particular, see Table IV in that appendix). We assume that DR units are unable to provide reactive power regulation. The regulation offer prices of all resources are given in the online appendix C [26]. For simplicity, we assume zero reactive loads in the illustrative example, though the large case study includes reactive loads. The upper and lower bounds of the nodal voltage magnitudes are set to 0.9 and 1.1 p.u., respectively. The voltage drop in this test case is very high, such that any differences between the three OPF models will be highlighted.

1) Results obtained from MILP-OPF (lossless): Since losses are not accounted for, the regulation sources on the two sides of the congested line between nodes 3 and 4 are *symmetrically*[9] re-dispatched, in such a way that the congestion is relieved. The regulation sources located at the PCC side of the congested line are TSO, DR unit c_1 and local generator i_1 (the so-called upstream sources), while the opposite side contains generator i_2, DR units c_2 and c_3 (downstream sources). The outcomes of the proposed DSO-level congestion management mechanism based on MILP-OPF (lossless) is depicted in Fig. 3a. Accordingly, in the time period with congestion (i.e., from time step 12 to 26), the downstream sources c_2 , c_3 and i_2 provide up-regulation while the upstream source with the best offer, i.e., TSO, provides down-regulation. In this time period, DR unit c_2 provides up-regulation through its rebound block, preceded with a response (down-regulation) before the congestion period. In contrast, DR unit c_3 provides up-regulation as its response block in the time period during congestion, and rebounds with down-regulation after the congestion. The total re-dispatch cost of the system, i.e., the value of objective function (5), is \$45.35.

2) Results obtained from iterative MILP-OPF with losses: We solve the iterative problem (9), which converges in the fourth iteration for this illustrative example. The congestion mechanism outcomes based on this iterative OPF problem is

[9]At any time step, the total up-regulation is equal to total down-regulation.

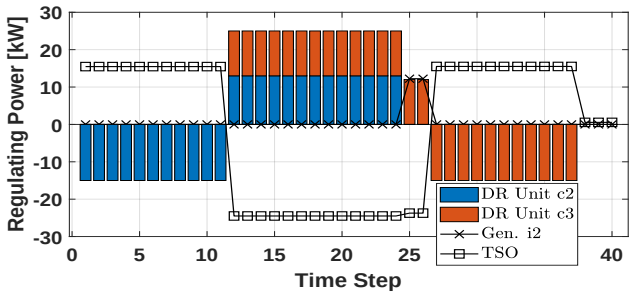

(a) MILP-OPF, lossless (total re-dispatch cost: \$45.35)

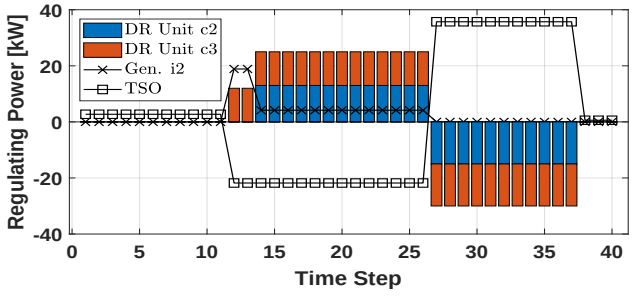

(b) MILP-OPF with losses (total re-dispatch cost: \$93.69)

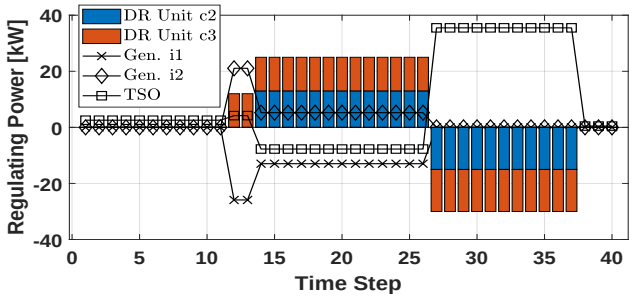

(c) MI-SOCP OPF with sufficient conditions (total re-dispatch cost: \$122.59)

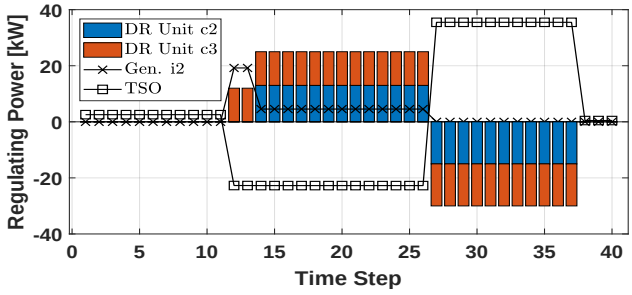

(d) MI-SOCP OPF without sufficient conditions (total re-dispatch cost: \$92.24)

Fig. 3. Illustrative example: Optimal active power regulation obtained from different congestion management mechanisms proposed.

given in Fig. 3b. Compared to Fig. 3a (the MILP-OPF without losses), we observe three main differences: i) a different asymmetric block offer from the down-stream DR unit c_2 is accepted, ii) due to active power losses[10], the total up- and down-regulations at each time step are not equal anymore, iii) the total re-dispatch cost of the system increases by \$48.34 (an increase of 106%).

[10]The reactive power losses are not modeled, but will be taken into account in MI-SOCP OPF model.

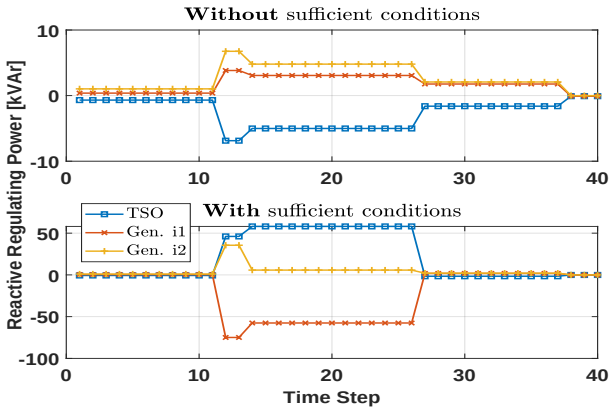

Fig. 4. Illustrative example: Optimal reactive power regulation obtained from the congestion management mechanism based on MI-SOCP OPF (upper plot: without sufficient conditions; lower plot: with sufficient conditions).

3) Results obtained from MI-SOCP OPF: This OPF model formulated in (10) is more precise than the two previous OPF models, as it considers both active and reactive power losses. Besides, voltages are modeled more precisely due to current magnitude modeling. Here, we provide results obtained from MI-SOCP OPF with and without enforcing the sufficient conditions for exactness. The active power re-dispatch results are given in Figs. 3c and 3d for cases with and without the sufficient conditions, respectively. For the same two cases, Fig. 4 depicts the reactive power re-dispatch results. There are three important observations to highlight.

First, the re-dispatch outcomes without sufficient conditions are found to be binding in (10b), which means that the convex relaxation is exact, and the solution achieved is AC feasible. The validation results that will be provided in Section IV.A.4 also confirm the exactness. However, note that this is case-specific, and in general, there is no guarantee achieving the exact solution from this relaxed OPF model without enforcing the sufficient conditions.

Second, the active power re-dispatch outcomes and the total re-dispatch cost obtained from MI-SOCP OPF model without sufficient conditions in Fig. 3d are similar to those obtained from the MILP-OPF model with losses in Fig. 3b. However, the voltage profile obtained in the MILP-OPF model with losses is not as accurate as the one in the MI-SOCP OPF model, as it will be demonstrated in Section IV.A.4.

Third, the total re-dispatch cost obtained from the MI-SOCP OPF model increases from \$92.24 to \$122.59 when adding the sufficient conditions. The reason for this cost increase is that the sufficient conditions shrink the feasible space. In other words, the MI-SOCP OPF model with sufficient conditions determines the exact optimal solution for the AC-OPF problem with the reduced feasible space. For example, these conditions avoid having simultaneous reverse active and reactive power flows, as demonstrated in Fig. 5 for a sample line. In the upper plot of this figure (without sufficient conditions), there are simultaneous reverse active and reactive power flows over the line from time step 12 to 26 (i.e., peak time period), while it never happens in the lower plot when adding sufficient conditions. For the same reason, the expensive generator i_1 is re-dispatched when enforcing sufficient conditions (Fig. 3c),

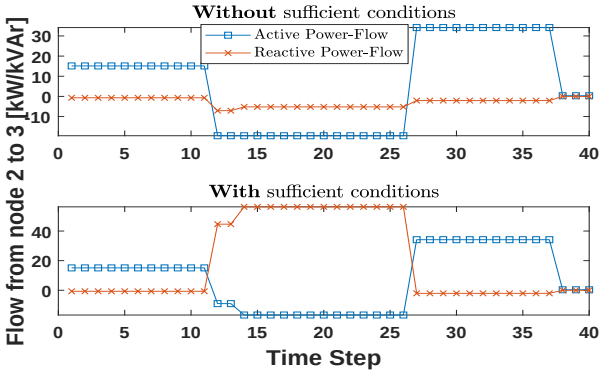

Fig. 5. Active and reactive power flow over the line from node n_2 to node n_3 (upper plot: without sufficient conditions; lower plot: with sufficient conditions).

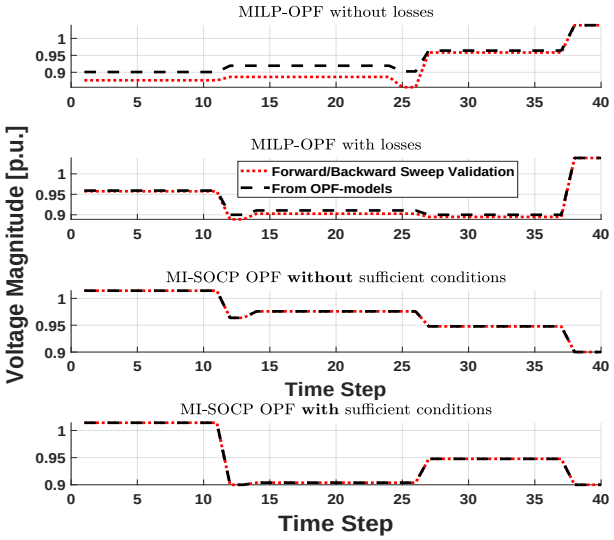

Fig. 6. Illustrative example: Voltage profile at node n_6 achieved by OPF models and forward-backward sweep validation (first plot: MILP-OPF lossless; second plot: MILP-OPF with losses; third plot: MI-SOCP OPF without sufficient conditions; fourth plot: MI-SOCP OPF with sufficient conditions).

while the production of that generator is unchanged in the case without sufficient conditions, and the TSO provides the regulation service instead (Fig. 3d). Therefore, it is logical to first check the exactness of the results obtained by MI-SOCP OPF model without sufficient conditions, and then to add those conditions if necessary.

4) Ex-post numerical validation: For given active and reactive regulation outcomes of flexible resources within the three different OPF models, we solve a power flow problem based on a forward-backward sweep method for validation purposes. This way, we numerically determine the voltage profiles at non-slack nodes (i.e., n_2 to n_6 as PQ nodes), and compare them with those achieved from the OPF models. Fig. 6 illustrates the voltage profile of node n_6 achieved from each OPF model and forward-backward sweep validation[11]. Based on the validation, as expected, the MI-SOCP OPF model provides the most precise outcomes. The error

[11]Node n_6 is selected since it is at the end of the feeder and thus is expected to have the most critical voltage profile.

is 0.0001% for the voltage of the worst node (n_6) when comparing the voltage profile obtained by forward-backward sweep validation method with that obtained from the MI-SOCP OPF model. This error in MILP-OPF models without and with losses is 2.4% and 0.55%, respectively. As another important observation, the voltage profiles obtained by the two MILP-OPF models are within the allowable bounds, however when verifying them with forward-backward sweep validation, it becomes apparent that the voltage constraints are violated in some time steps. However, this is not the case for the voltage profiles obtained from MI-SOCP OPF model with and without sufficient conditions, which verifies their solution is AC feasible and exact.

B. Case Study: IEEE 37-Node Test Feeder

For the case study, we use the IEEE 37-node test-feeder [32], whose diagram is given in the online appendix D [26]. All three-phase line impedances and loads are transformed into single phase equivalents, and transformers are removed where necessary. The load data profiles are generated with 30-minute time resolution, yielding a time horizon with 48 time steps. The spot loads of the original test case are considered as the peak load magnitudes, and then the 24-hour load profiles are normalized based on data for a summer week-day in 2017 for eastern Denmark sector of the Nordpool market. Load curves are given in the online appendix D [26]. Five conventional generators and four DR units are located at different nodes. The line capacity between nodes 2 and 3 is limited to 1000 kVA, such that it will be congested during the peak load hours.

For computational performance analysis, we consider two cases, namely Cases A and B, with different number of offers per DR unit and thus different number of binary variables in the OPF models. In Case A, each DR unit submits three asymmetric block offers, while it is 8 offers in Case B. In particular, Case A ends up to mixed-integer models with 576 binary variables, while Case B contains 1536 binary variables.

Fig. 7 presents the voltage profile in Case A for the worst node achieved from the three OPF models and the forward-backward sweep validation. Similar to our results in the illustrative example, MI-SOCP OPF provides more precise outcomes than the other two MILP models. Some extra results are available in the online appendix [26].

The total re-dispatch cost, total active and reactive power losses and CPU times[12] among the three OPF models are given in Table I. In particular, note that this table includes the results obtained from the MI-SOCP OPF with and without sufficient conditions. Similar to the illustrative example in the previous section, the MI-SOCP OPF model without sufficient conditions is found to be binding in the second-order cone constraint (10b). This implies that the solution of the MI-SOCP OPF model in this specific case study is exact and thus AC feasible. In Case A, compared to the MI-SOCP OPF without sufficient conditions, the MILP-OPF with loss approximation underestimates the total active power losses and the total re-dispatch cost by 8.7% and 12.3%, respectively.

[12]Hardware used: Huawei XH620 V3 with two Intel Xeon Processors 2650v4 (12 core, 2.20GHz), 256 GB memory, FDR Infiniband, 480 GB-SSD disk

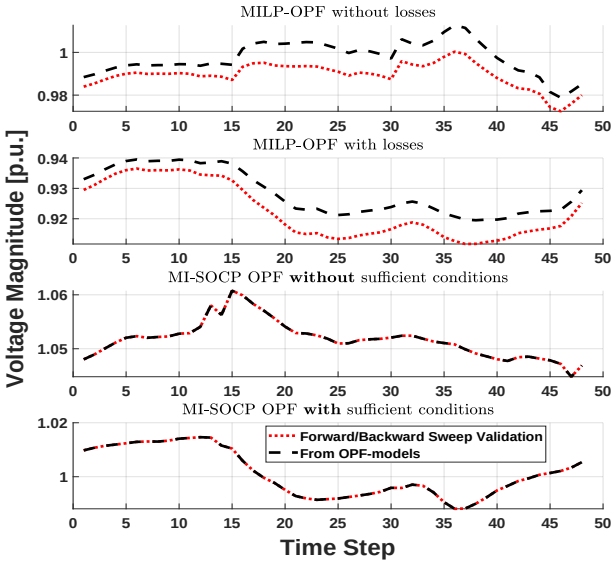

Fig. 7. Case study (Case A): Voltage profile at node n_{32} achieved by OPF models and forward-backward sweep validation (first plot: MILP-OPF lossless; second plot: MILP-OPF with losses; third plot: MI-SOCP OPF without sufficient conditions; fourth plot: MI-SOCP OPF with sufficient conditions).

TABLE I
CASE STUDY: OUTCOMES OF THE THREE PROPOSED CONGESTION MANAGEMENT MECHANISMS AND THEIR CPU TIMES FOR CASES A AND B

Result	Case	MILP lossless	MILP w. loss	MISOCP w. suff.	MISOCP w/o. suff.
Re-dispatch cost [$]	A	1694	2486	5115	2836
Active loss [kWh]		N/A	1454	2819	1593
Reactive loss [kVArh]		N/A	N/A	1913	1379
CPU time [s]		9	72.9	513	288
Re-dispatch cost [$]	B	1594	2371	5007	2725
Active loss [kWh]		N/A	1478	2783	1607
Reactive loss [kVArh]		N/A	N/A	1896	1384
CPU time [s]		34	209	12478	1381

These underestimations in Case B are 8.0% and 13.0%, respectively. When adding sufficient conditions to the MI-SOCP OPF model, the system cost increases significantly. The reason for this cost increase is that the sufficient conditions shrink the feasible space, and consequently, some expensive up-stream generators (closer to the PCC) are re-dispatched. This conic model as the most accurate mechanism among the three models requires more CPU time than the other two MILP mechanisms. The increase in CPU time by increasing the number of binary variables, especially in MI-SOCP OPF model with sufficient conditions, is significant. The CPU time increase is less significant when no sufficient conditions are enforced. In order to get a better insight into the increase in CPU time versus the amount of binary variables in the MI-SOCP OPF model with sufficient conditions, we plot the CPU time as a function of numbers of time steps and asymmetric block offers in Fig. 8.

V. CONCLUSION

This paper proposed a congestion management mechanism for distributions grids, accounting for potential rebound effect of demand response units. To this purpose, we incorporated

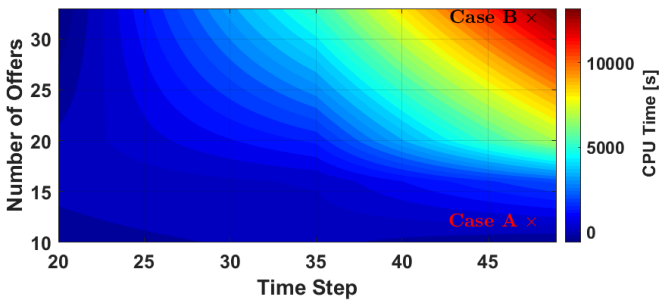

Fig. 8. Case study: CPU time for the MI-SOCP OPF model with sufficient conditions as function of time steps and total number of block offers. (Note: this is a linear interpolation between at 24, 35 and 48 time steps, and 12, 16, 20 and 32 offers.)

asymmetric block offers into the proposed mechanism at the cost of introducing a set of binary variables, which leads to increasing computational burden. For this mechanism, we checked three different OPF models: i) MILP-OPF (lossless) as the most simplified one, ii) MILP-OPF with loss approximations, and iii) MI-SOCP OPF as the most accurate one. We also analyze the performance of MI-SOCP OPF model with and without including sufficient conditions that guarantee an exact relaxation (i.e. AC feasible solution). We show that the outcomes of the proposed mechanism, especially asymmetric blocks dispatched, are sensitive to the OPF model used, i.e., the level of network simplifications considered. Among the three models, the MI-SOCP OPF has the best technical performance, but at the cost of high computational burden, especially when adding sufficient conditions for exactness. It is of our future interest to explore the alternatives to reduce the computational burden, e.g., using decomposition techniques.

REFERENCES

[1] J. Villar, R. Bessa, and M. Matos, "Flexibility products and markets: Literature review," *Electr. Power Syst. Res.*, vol. 154, pp. 329–340, 2018.

[2] S. Y. Hadush and L. Meeus, "DSO-TSO cooperation issues and solutions for distribution grid congestion management," *Energy Policy*, vol. 120, pp. 610–621, 2018.

[3] F. Capitanescu, "TSO–DSO interaction: Active distribution network power chart for TSO ancillary services provision," *Elect. Power Syst. Res.*, vol. 163, pp. 226–230, 2018.

[4] M. Caramanis, E. Ntakou, W. W. Hogan, A. Chakrabortty, and C. Schoene, "Co-optimization of power and reserves in dynamic T&D power markets with nondispatchable renewable generation and distributed energy resources," *Proceedings of the IEEE*, vol. 104, no. 4, pp. 807–836, 2016.

[5] A. Papavasiliou and I. Mezghani, "Coordination schemes for the integration of transmission and distribution system operations," in *Power Syst. Comput. Conf. (PSCC)*, (Dublin, Ireland), Jun. 2018.

[6] A. Vicente-Pastor, J. Nieto-Martin, D. W. Bunn, and A. Laur, "Evaluation of flexibility markets for retailer-DSO-TSO coordination," *IEEE Trans. Power Syst.*, 2018, to be published.

[7] J. P. Silva, J. A. Sumaili, R. J. Bessa, L. Seca, M. A. Matos, V. Miranda, M. Caujolle, B. Goncer-Maraver, and M. Sebastian-Viana, "Estimating the active and reactive power flexibility area at the TSO-DSO interface," *IEEE Trans. Power Syst.*, vol. 33, no. 5, pp. 4741–4750, 2018.

[8] R. A. Verzijlbergh, L. J. De Vries, and Z. Lukszo, "Renewable energy sources and responsive demand. Do we need congestion management in the distribution grid?" *IEEE Trans. Power Syst.*, vol. 29, no. 5, pp. 2119–2128, 2014.

[9] L. A. Greening, D. L. Greene, and C. Difiglio, "Energy efficiency and consumption—the rebound effect—a survey," *Energy Policy*, vol. 28, pp. 389–401, 2000.

[10] S. Sorrell and J. Dimitropoulos, "The rebound effect: Microeconomic definitions, limitations and extensions," *Ecological Economics*, vol. 65, pp. 636–649, 2008.

[11] F. Sossan, *Indirect control of flexible demand for power system applications*. (Ph.D. thesis), Technical University of Denmark, 2014. [Online]. Available: http://orbit.dtu.dk/files/100219481/sossan_thesis.pdf.

[12] Y. Liu, J. T. Holzer, and M. C. Ferris, "Extending the bidding format to promote demand response," *Energy Policy*, vol. 86, pp. 82–92, 2015.

[13] N. O'Connell, P. Pinson, H. Madsen, and M. O'Malley, "Economic dispatch of demand response balancing through asymmetric block offers," *IEEE Trans. Power Syst.*, vol. 31, no. 4, pp. 2999–3007, 2016.

[14] G. A. Dourbois, P. Biskas, and D. I. Chatzigiannis, "Novel approaches for the clearing of the European day-ahead electricity market," *IEEE Trans. Power Syst.*, vol. 33, no. 6, pp. 5820–5831, 2018.

[15] N. O'Connell, Q. Wu, J. Østergaard, A. H. Nielsen, S. T. Cha, and Y. Ding, "Day-ahead tariffs for the alleviation of distribution grid congestion from electric vehicles," *Electr. Power Syst. Res.*, vol. 92, pp. 106–114, 2012.

[16] S. Huang, Q. Wu, S. S. Oren, R. Li, and Z. Liu, "Distribution locational marginal pricing through quadratic programming for congestion management in distribution networks," *IEEE Trans. Power Syst.*, vol. 30, pp. 2170–2178, 2015.

[17] R. Li, Q. Wu, and S. S. Oren, "Distribution locational marginal pricing for optimal electric vehicle charging management," *IEEE Trans. Power Syst.*, vol. 29, no. 1, pp. 203–211, 2014.

[18] H. Zhong, L. Xie, and Q. Xia, "Coupon incentive-based demand response: Theory and case study," *IEEE Trans. Power Syst.*, vol. 28, no. 2, pp. 1266–1276, 2013.

[19] M. R. Sarker, M. A. Ortega-Vazquez, and D. S. Kirschen, "Optimal coordination and scheduling of demand response via monetary incentives," *IEEE Trans. Smart Grid*, vol. 6, no. 3, pp. 1341–1352, 2015.

[20] S. Huang and Q. Wu, "Real-time congestion management in distribution networks by flexible demand swap," *IEEE Trans. Smart Grid*, vol. 9, no. 5, pp. 4346–4355, 2018.

[21] S. Huang, Q. Wu, J. Wang, and H. Zhao, "A sufficient condition on convex relaxation of AC optimal power flow in distribution networks," *IEEE Trans. Power Syst.*, vol. 32, no. 2, pp. 1359–1368, 2017.

[22] S. H. Low, "Convex relaxation of optimal power flow—Part I: Formulations and equivalence," *IEEE Trans. Control Netw. Syst.*, vol. 1, no. 1, pp. 15–27, 2014.

[23] M. Nick, R. Cherkaoui, J.-Y. Le Boudec, and M. Paolone, "An exact convex formulation of the optimal power flow in radial distribution networks including transverse components," *IEEE Trans. Autom. Control*, vol. 63, pp. 682–697, 2018.

[24] L. Bobo, S. Delikaraoglou, N. Vespermann, J. Kazempour, and P. Pinson, "Offering strategy of a flexibility aggregator in a balancing market using asymmetric block offers," in *Power Syst. Comput. Conf. (PSCC)*, (Dublin, Ireland), Jun. 2018.

[25] N. O'Connell, H. Madsen, P. Pinson, M. O'Malley, and T. Green, "Regulating power from supermarket refrigeration," in *Innovative Smart Grid Technologies Conference Europe (ISGT-Europe)*, (Istanbul, Turkey), IEEE, 2014, pp. 1–6.

[26] *Online appendix*. [Online]. Available: https://github.com/alherm/asymmetric_block_offers (visited on 07/30/2018).

[27] A. Helseth, "A linear optimal power flow model considering nodal distribution of losses," in *Conf. on the European Energy Market (EEM)*, (Florence), 2012.

[28] B. Eldridge, R. O'Neill, and A. Castillo, "An improved method for the DCOPF with losses," *IEEE Trans. Power Syst.*, vol. 33, no. 4, pp. 3779–3788, 2018.

[29] J. A. Taylor, *Convex Optimization of Power Systems*. Cambridge University Press, 2015.

[30] P. Sulc, S. Backhaus, and M. Chertkov, "Optimal distributed control of reactive power via the alternating direction method of multipliers," *IEEE Trans. Energy Convers.*, vol. 29, no. 4, pp. 968–977, 2014.

[31] L. Halilbasic, P. Pinson, and S. Chatzivasileiadis, "Convex relaxations and approximations of chance-constrained AC-OPF problems," *IEEE Trans. Power Syst.*, 2018, to be published.

[32] *37-bus feeder*, IEEE, 2000. [Online]. Available: http://sites.ieee.org/pes-testfeeders/resources/ (visited on 04/17/2018).